

Behavior of Reinforced Sand Subjected to Shear along Vertical Plane

Rajashekar M Hubballi

A Dissertation Submitted to
Indian Institute of Technology Hyderabad
In Partial Fulfillment of the Requirements for
The Degree of Master of Technology



भारतीय प्रौद्योगिकी संस्थान हैदराबाद
Indian Institute of Technology Hyderabad

Department of Civil Engineering

July, 2013

Declaration

I declare that this written submission represents my ideas in my own words, and where others' ideas or words have been included, I have adequately cited and referenced the original sources. I also declare that I have adhered to all principles of academic honesty and integrity and have not misrepresented or fabricated or falsified any idea/data/fact/source in my submission. I understand that any violation of the above will be a cause for disciplinary action by the Institute and can also evoke penal action from the sources that have thus not been properly cited, or from whom proper permission has not been taken when needed.

R. M. Hubballi

(Signature)

Rajashekar M Hubballi

(Student Name)

CE11M07

(Roll No)

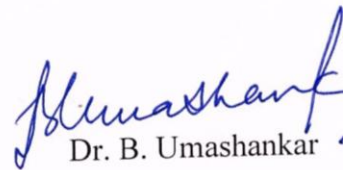
Approval Sheet

This thesis entitled “Behavior of Reinforced Sand Subjected to Shear along Vertical Plane” by Rajashekar M Hubballi is approved for the degree of Master of Technology from IIT Hyderabad.



Dr. Raja Banerjee
Assistant Professor
Department of Mechanical Engineering
Examiner

Dr. K.B.V.N. Phanindra
Assistant Professor
Department of Mechanical Engineering
Examiner



Dr. B. Umashankar
Assistant Professor
Department of Mechanical Engineering
Adviser

Acknowledgements

I gratefully acknowledge all the valuable help, advice and motivation from Dr. Umashankar Balunaini, who guided me in carrying out this thesis work. I wish to express my gratitude and most sincere thanks to Prof. Madhav R Madhira for his valuable suggestions, supervisions and enthusiasm in all aspects of this work. I would like to express my gratitude to all the faculty members in the Civil Engineering Department for making my M. Tech program a good and memorable experience.

I am also very grateful to my family for their support in all aspects. I am thankful to all my friends and my classmates who always have supported and encouraged me.

My special thanks to Hariprasad C, Suraj Vedpathak, Saranya Selvam and Sasanka Mouli for their help and support during my M. Tech program.

Dedicated to

My Parents

Abstract

For proper design of any reinforced structure, soil-reinforcement interaction should be determined. The pullout resistance of the reinforcement is an important parameter in the design of reinforced earth structures. The existing design procedures consider the pullout resistance due to only axial pull. However, the kinematics of failure clearly establishes that the reinforcement is displaced obliquely. This work presents the results of reinforced soil bed when sheared normal to the reinforcement. Tests materials included sand and several soil reinforcements like strips, geogrids, etc. The shear stress-displacement responses at various normal stresses are presented and test results show that the shear resistance of reinforced sand under normal shear is significantly higher than that of unreinforced sand. Plots are provided showing the comparison of the shear stress-displacement response of reinforced and unreinforced beds under the test conditions proposed in the study.

Contents

| | |
|--|-------------------------------------|
| Declaration..... | E |
| Error! Bookmark not defined. | |
| Approval Sheet..... | Error! Bookmark not defined. |
| Acknowledgements..... | iv |
| Abstract..... | vi |
| 1 Introduction..... | 1 |
| 1.1 Overview..... | Error! Bookmark not defined. |
| 1.2 Objectives of the study..... | 7 |
| 1.3 Organization of the study..... | 7 |
| 2 Literature Review..... | 8 |
| 2.1 Introduction..... | 8 |
| 2.2 Analysis of Reinforced Earth subjected to Pull out force | 9 |
| 3 Materials Properties..... | 16 |
| 3.1 Introduction..... | 16 |
| 3.2 Characteristics of Sand..... | 16 |
| 3.2.1 Sieve Analysis..... | 16 |
| 3.2.2 Specific Gravity | 17 |
| 3.2.3 Maximum and Minimum dry densities | 17 |
| 3.2.4 Direct shear test..... | 17 |
| 3.3 Reinforcement Characteristics | 19 |
| 3.3.1 Geogrid | 19 |
| 3.3.2 Paraweb Strip | 20 |
| 3.4 Interface Direct Shear Test | 20 |
| 4 Test Methodology | 22 |
| 4.1 Introduction..... | 22 |
| 4.2 Test setup | 22 |
| 4.2.1 Shear Box..... | 22 |
| 4.2.2 Springs | 27 |
| 4.2.3 Dial Gauges..... | 28 |
| 4.2.4 Hydraulic Jack with Proving ring | 28 |
| 4.3 Sample Preparation | 29 |
| 4.3.1 Compactor..... | 29 |

| | | |
|---------------------------------------|-------------------------------------|-----------|
| 4.3.2 | Geogrid reinforced sand..... | 31 |
| 4.3.3 | Paraweb Strips reinforced sand..... | 32 |
| 4.4 | Test Procedure..... | 32 |
| 5.Results and Conclusions..... | | 34 |
| 5.1 | Introduction..... | 34 |
| 5.2 | Unreinforced Sand | 34 |
| 5.3 | Reinforced Sand..... | 38 |
| 5.4 | Conclusions..... | 41 |
| References..... | | 42 |

Chapter 1

Introduction

1.1 Overview

Transportation plays a major role in the development of human civilization. Among different modes of transportation, road and railways are most commonly preferred. While constructing roads and railways, earthen embankments are often used to maintain the required level. Poor design and construction of such earthen embankments may lead to their failure. Figure 1.1 shows one such embankment failure.



Figure 1.1: Failure of Highway 101 road embankment, Olympia, USA [1].

Highway 101 earthen road embankment is located near state road 8 junction, Olympia, USA. The embankment crosses a ravine that was carrying water at the time of failure. The embankment is about 15 to 20 m high, has a crest width of 30 m and has side slopes of approximately 1.5H:1V. A 1 m diameter corrugated metal culvert through the base of the embankment provides drainage across it. The failed material flowed down slope approximately 150 m and partially covered the road that parallels Highway 101 to the north. Pavement sections and culvert materials were found about 50 m and 70 m, respectively, north of the edge of the original road embankment (GPS N47.05834 W123.01365; 03/03/01) [1].



**Figure 1.2: Failure of Earthen Embankment in Woo-wan-chai Area,
Mt. Ali Road, Taiwan [2]**

Figure 1.2 shows the failure in embankment soil that occurred in 2003 in Woo-wan-chai Area, Mt. Ali Road, Taiwan. Mt. Ali Road (also known as Province Road 18) provides main access to Yushan National Park of Taiwan and is a Alishan National Scenic Area. An old land slide area, Woo-wan-chai covers an area of about 50 ha and located at a mileage of about 30 km along the road. On 26th of June, 2003, a major slope failure occurred in the area with estimated volume of about 50,000 cubic meter and resulted in serious damage to the road and the local traffic [2].

Such failures in earthen embankments may occur due to excessive settlement or shear failure. Shear failure occurs when the shear stress acting along the slip surface exceeds the shear strength of the soil. To build safe, economical and durable earth retaining structures, an innovative approach known as Reinforced soil construction is resorted to. Reinforced soil engineering originated from France. First retaining wall of reinforced soil in the World was built in France in 1965. In this technique, the properties of soil mass are improved by incorporating strips of suitable reinforcing material. Various reinforcing materials such as Geogrids, Pareweb strips, Geocells, Geotextiles, etc. (Figure 1.3) are used to reinforce steep slopes, retaining structures and embankments, as shown in Figure 1.4.

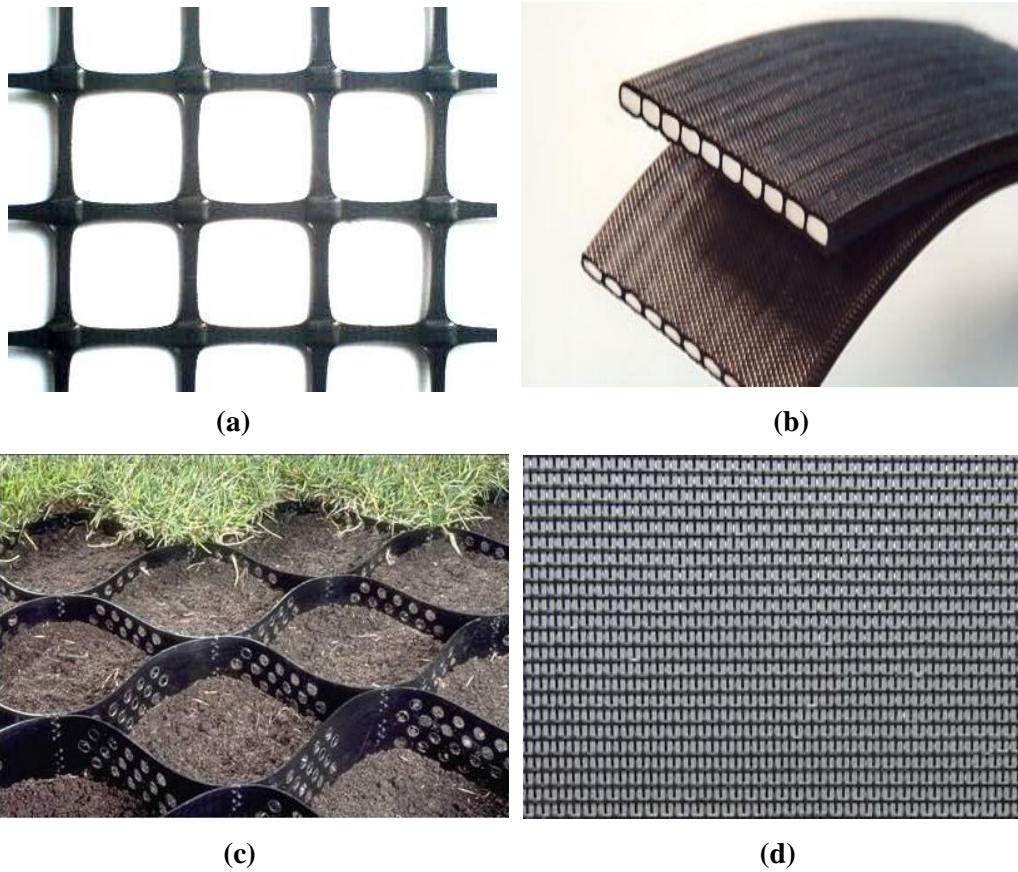


Figure 1.3: Reinforcing Materials: (a) Geogrid, (b) Paraweb strip, (c) Geocell, and (d) Geotextile

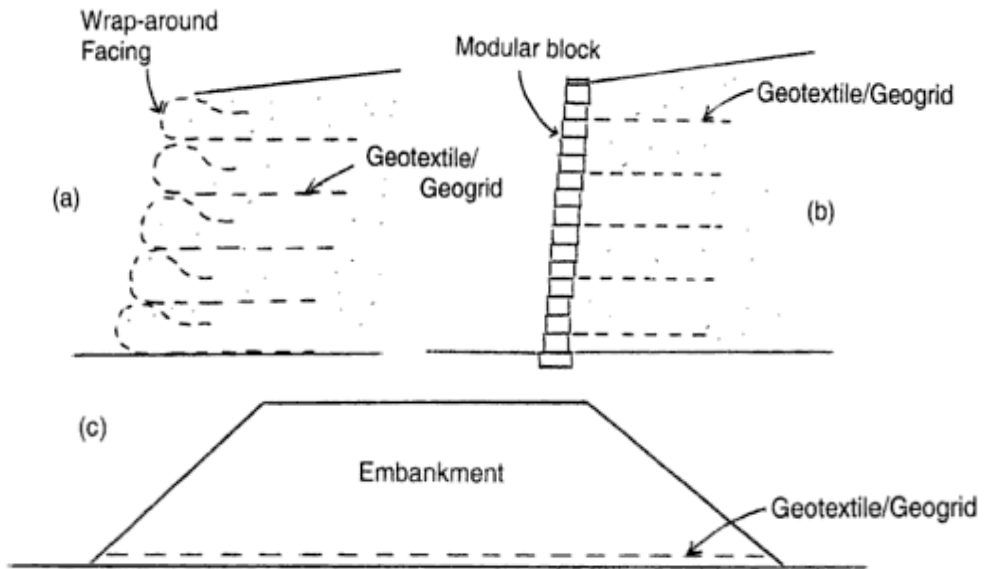


Figure 1.4: Reinforced structures: (a) Steep Slope, (b) Retaining Wall, and (c) Embankment [3]

Reinforced earth is built in stages, each stage consisting of the assembly of a new layer of facing elements and the placing of the corresponding earth fill, followed by a new layer of reinforcing strips. Certain minimum criteria with respect to grading and water content should be met in order to ensure development of sufficient friction between the earth and reinforcement. The length of the strip depends on the internal stability of the reinforced earth mass. These strips will usually be tied to the facing of the embankment. Facing is the covering used to protect the front of the soil mass. This can consist of any material, but concrete panels are commonly used. The purpose of the facing is to retain the soil between the layers of reinforcement in the immediate vicinity of the wall facing. Compaction is necessary whenever there is a need to minimise settlement of the reinforced structure, for example, to support a highway or to carry concentrated loads [3].

The mechanism of unreinforced and reinforced soils can be explained by considering an element of soil along the slip surface, as shown in Figure 1.5. The shear resistance mobilized along the slip surface of an unreinforced soil can be determined by preparing the sample in a direct shear box in the laboratory (Figure 1.6).

From Figure 1.6, it is apparent that the shear resistance that can develop on a failure surface is given by

$$P_{\text{resisting}} = P_v \tan\phi \quad (1.1)$$

where, P_v is the vertical load in the shear box or the normal load on the failure surface in an unreinforced slope, ϕ is the angle of shearing resistance of soil, and $P_{\text{resisting}}$ is the resisting force acting along the failure surface in the shear box or in an unreinforced slope.

Similarly, for a reinforced soil element, it can be seen from the kinematics of deformation of soil element along the slip surface that the reinforcement is sheared at an angle, θ , with the horizontal (Figure 1.5). Figure 1.7 shows the corresponding direct shear box analogy.

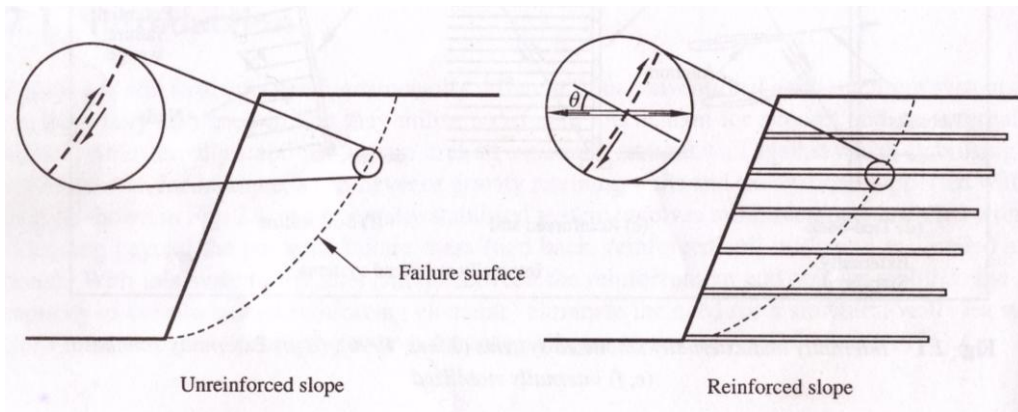


Figure 1.5: Steep slopes: Unreinforced and Reinforced [4]

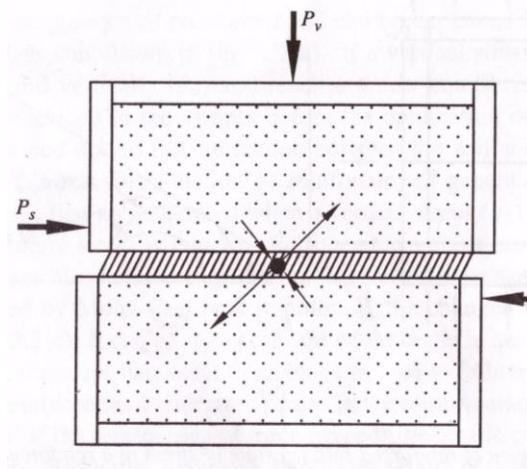


Figure 1.6: Idealised failure element in Unreinforced slope [5]

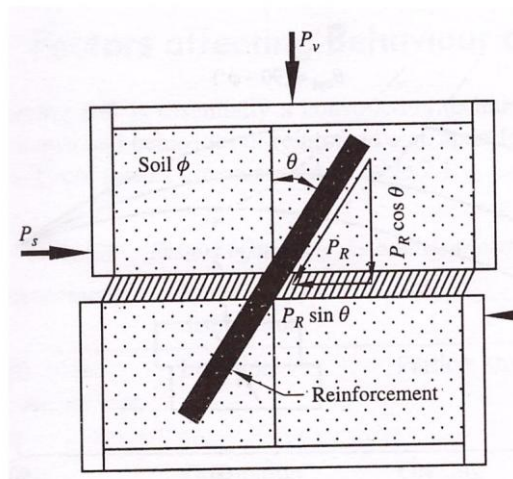


Figure 1.7: Idealised failure element in reinforced slope [5]

From Figure 1.7, the shear resistance that can develop on a failure surface is given by

$$P_{\text{resisting}} = P_v \tan\phi + P_R (\sin\theta + \cos\theta \tan\phi)$$

where, P_R the is force along reinforcement.

From the resolution of forces within the reinforcement and shearing soil element, it can be seen that the reinforcement has two beneficial effects on the shear resistance of the reinforced soil mass.

1. There is a reduction in the shear force through the horizontal component of the tensile force in the reinforcement.
2. There is an increase in the normal force applied to the shear surface, and hence an associated increase in the shear resistance derived from the vertical component of the tensile force in the reinforcement.

Hence soil reinforcements play a crucial role in minimizing the shear failure of soils and in reducing the settlement. While designing the reinforced slopes, axial pull out is assumed to have developed along the reinforcement. However, kinematics of slope failure establishes that the reinforcement is pulled normally and obliquely (Fig. 1.8) along the slip surface.

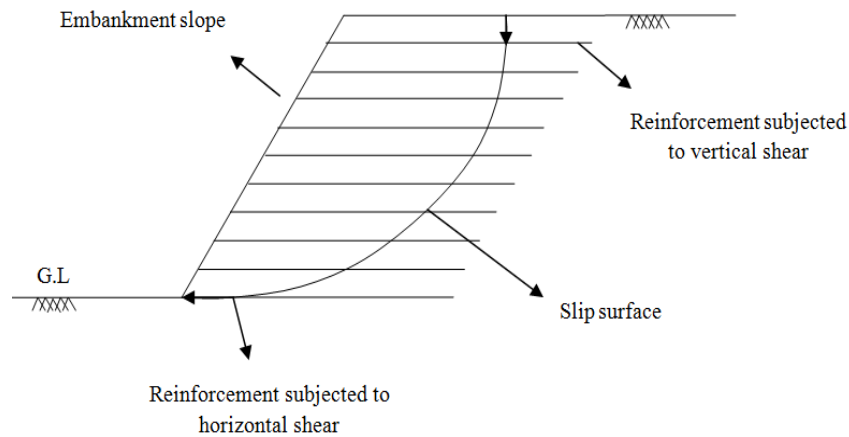


Figure 1.8: Reinforcement subjected to pull inclined at different inclinations with the horizontal

This thesis aims at studying the behavior of reinforcements in the slopes which are subjected to normal pull (Figure 1.9). To replicate this, a new pattern of direct shear apparatus is designed. Reinforced soil in the direct shear box is subjected to shear in a vertical plane to understand its response to normal pull.

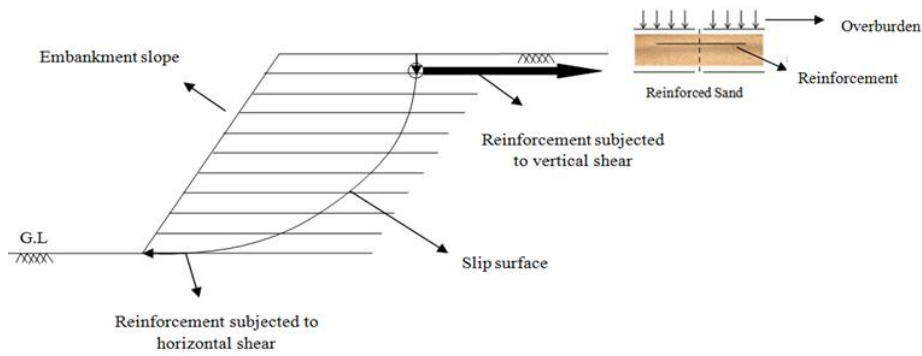


Figure 1.9: Reinforcements in Slopes subjected to normal pull

1.2 Objectives of the study

The objectives of this study are:

- ❖ To obtain the angle of shearing resistance of reinforced soil when shearing is along vertical plane.
- ❖ To compare the shear stress vs. displacement response along the vertical plane under different normal stresses for unreinforced and reinforced soils.

1.3 Organization of the study

This thesis has been divided into five Chapters. Chapter-1 provides an Overview and Objectives of the study. Theoretical background related to the research work is discussed in this Chapter. Chapter-2 provides a review of studies available in the literature on related topic.. Chapter-3 discusses the characteristics of Soil and Reinforcement used in the present study. It discusses various tests performed on soil and reinforcement along with the test results. Chapter-4 discusses test methodology which includes test setup, sample preparation and test procedure. Test set up discusses in detail the apparatus used for testing, various accessories connected with the apparatus, their arrangement, position, etc. Sample preparation explains the method followed for preparing sand beds. Test procedure discusses method of carrying out the test step by step. Finally, Chapter-5 discusses the test results and conclusions.

Chapter 2

Literature Review

2.1 Introduction

Reinforced earth structures such as reinforced embankments, retaining walls, subgrades below the pavements, etc., are becoming popular with time because of their ability to withstand more load, large displacements and perform better under seismic conditions. The interaction mechanism between reinforcement and soil is of two types, namely, direct shear mechanism and pull out mechanism (Figure 2.1). In the Figure below, the sliding wedge passes through the reinforcements, subjecting the top layers of the reinforcement to pull out force and lower layers of the reinforcement to sliding against the fill material.

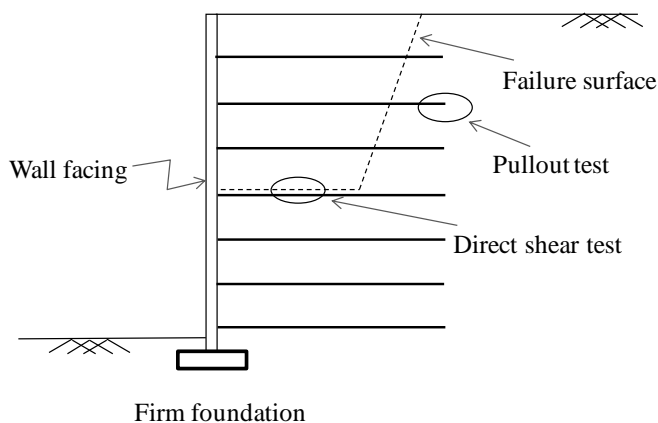


Figure 2.1: Soil-reinforcement interaction [6]

For each of possible mechanisms of internal collapse in the reinforced soil embankment, reinforcement interacts with soil in a different way (Figure 2.2). Different test procedures to study the soil and reinforcement interaction were developed depending on the failure mechanism. Sliding of soil above the surface of reinforcement in the *A zone* can be tested using a soil-reinforcement interface direct shear test. As soil and reinforcement move laterally in *zone B*, the suitable test will be tensile test. Direct shear

test with inclined reinforcement in relation to the shear plane present a simulation of the interaction mechanism that occurs in the *Zone C*. Pullout testing reproduces the mechanism appearing in the *Zone D* where the reinforcement pullout from soil occurs.

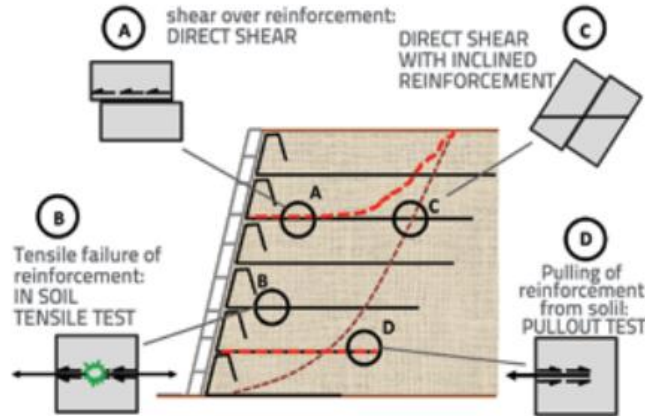


Figure 2.2: Cross section of reinforced embankment with failure mechanism and test that correspond to a particular failure mechanism [29].

In this Chapter, a review of previous research studies performed specific to response of reinforced earth to the pull out forces in various directions is presented.

2.2 Analysis of Reinforced Earth subjected to pull out force

Alfaro et al. (1995) conducted pull out test on geogrid embedded in dense granular soil subjecting the geogrid to horizontal pull out force (Figure 2.2).

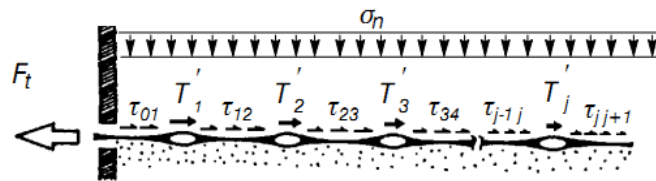


Figure 2.2: Geogrid subjected to horizontal pull out force

Geogrids used were uniaxial geogrids of various widths ranging from 0.2 m to 1 m. Results confirmed that a three dimensional interaction mechanism had developed at both edges of the reinforcement. This mechanism due to confinement of the dilating zone of soil around the reinforcement is also studied [23]. As the reinforcement is pulled out, shear displacement occurs along the interface and the zone of soil surrounding the reinforcement tends to dilate. However, the volume change is restrained by the surrounding non dilating soil, resulting in an increase in normal stress on the soil-reinforcement interface. Soil-reinforcement interaction mechanism for geogrids which

range in width from 0.2 m to 1 m is a combination of two dimensional interaction mechanism developing over the middle section and three dimensional interaction mechanism developing at edges. The contribution of 3-D interaction mechanisms is found to decrease with increase of normal stress. This confirmed that the 3-D interaction mechanism is a consequence of restrained dilatancy effect [22].

Lopes and Lopes (1999) presented the influence of soil particle size and geosynthetic structure on soil-geosynthetic interaction. Soil particles smaller than the geogrid aperture size can penetrate the geogrid, but are less effective in mobilizing the passive resistance in the bearing members. Soils with a significant percentage of particles larger than the geogrid aperture could lead to a worse situation because the particles cannot enter the apertures and would limit the mobilization of the soil-reinforcement interface skin friction at the contact points between soil particles and the planar surface of the reinforcement [30].

Bergado et al. (2000) conducted large direct shear test with inclined geotextile and hexagonal wire mesh reinforcements to investigate the mobilized inclination and reinforcement strain during shear near the failure surface using reinforcement of different stiffness.



Figure 2.3: Orientation of hexagonal wire mesh (a) before testing (b) after testing

The mobilized strain and orientation of reinforcement were presented as functions of shear displacements. The results showed that maximum orientation of the reinforcements are not greater than the bisecting direction and have not reached the tangential direction. The mobilized orientation of reinforcement force is observed to be independent of geotextile stiffness. For the same shear displacement, with the increase in geotextile stiffness, mobilized orientation of reinforcement force is found to have

decreased and increased slightly with increase of confining pressure. The slope of deformed hexagonal wire mesh and the geotextile reinforcement close to the slip surface were found to be similar and assumed to be parabolic [15].

Madhav and Umashankar (2003a) presented an analysis for the sheet reinforcement subjected to transverse force. A simple Winkler type response for the ground is assumed and inextensible reinforcement is used to estimate the resistance to transverse force. It is found that response to the applied force is a function of interface shear characteristics of the reinforcement and deformational response of the ground.

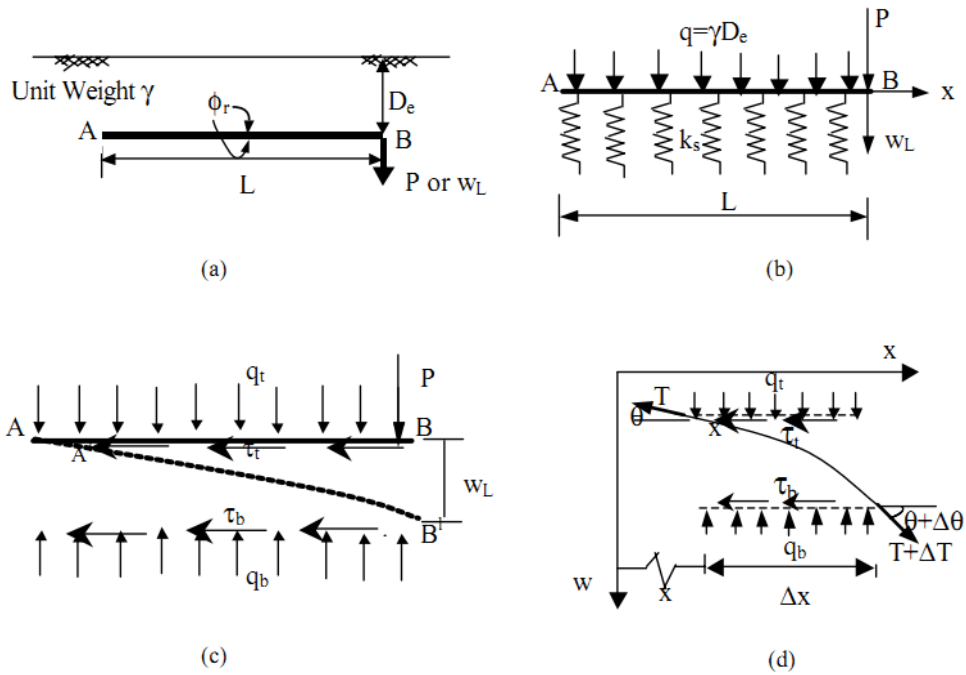


Figure 2.4: (a) Reinforcement subjected to transverse force, (b) Model, (c) Deformed profile and (d) Forces on an element.

A relation was established between pull-out resistance and transverse free-end displacement. It was showed that the reinforcement in dense granular fills subjected to a transverse pull generates pull-out resistance larger than purely axial pull-out capacity in reinforced earth construction. The normal stresses developed on the reinforcement-soil interface under the action of axial pull remain the same as the gravity stresses. As a result, shear resistance mobilized at the interface is proportional to these normal stresses. However, under the action of transverse force or displacement, the soil below the reinforcement mobilizes additional normal stresses as the reinforcement deforms transversely [16].

Madhav and Umashankar (2003b) presented the analysis of pull out resistance of sheet reinforcement subjected to transverse force and displacement assuming a non-linear subgrade or fill response and an inextensible reinforcement. The response to the applied force is found to be dependent not only on the interface shear characteristics of the reinforcement but also on the deformational response of the ground [20].

Shahu (2007) analyzed the pullout resistance of sheet reinforcement subjected to an oblique end force assuming a linear subgrade response and an inextensible reinforcement. It was observed that at high obliquities of the end force, increase in friction resistance due to the downward component of the end force becomes high. But the high obliquity also caused bending of the reinforcement which reduced the frictional resistance resulting in occurrence of pull out. For an obliquity of 60° and an angle of interface shearing resistance of 30° , the horizontal component of the oblique force was found to increase by 50% of the pure axial pullout capacity of the reinforcement. Thus the most important factors affecting the horizontal component of the pullout capacity are found to be obliquity of the end force and the interface angle of shearing resistance [24].

Chia-Nan et al. (2009) analyzed the behavior of geogrid-sand interface resistance in direct shear mode. Normal stresses of approximately 50 kPa, 100 kPa and 150 kPa were maintained in the test. Rate of horizontal displacement was maintained at 1 mm/min. The vertical displacement versus shear displacement curve obtained from the test showed that the geogrid-sand interface undergoes an initial vertical contraction for small values of shear displacement. The specimen exhibited dilatancy for larger values of shear displacement. A comparison with the vertical deformation behavior of pure sand showed that the geogrid-sand interface experiences comparatively smaller vertical displacement during shearing. Maximum dilatancy of the sand occurs at the shear displacement that corresponds to the yield shear stress rather than at the shear displacement that corresponds to the peak shear strength of the interface. Inspection of the shear displacement behavior of sand-geogrid interfaces provided evidence that passive resistance also contributes to the shear strength of sand-geogrid interface [28].

Bonod and Hadi (2010) analyzed the reinforced soil embedded with vertical reinforcement along with conventional horizontal reinforcement. There is an increase in load resisting capacity of reinforced earth because the placement of reinforcement

perpendicular to the shearing plane provides passive resistance against shearing, making all the layers intact that will increase the strength and stability of the reinforced soil. It was found that different modes of failure can be arrested with the use of vertical reinforcement along with horizontal reinforcement. Vertical reinforcement cages the soils in different units along with soil layered by horizontal reinforcement and produce intact effects in soil mass. Horizontal reinforcement enhances the tensile strength and provides bending effects. Vertical reinforcement reduces the induced tensile stresses in horizontal reinforcement resulting in less length [18].

Patra and shahu (2011) presented the effect of subgrade shear stiffness on oblique pullout behavior of reinforced soil. Effect of shear stiffness on the displacement profile is such that with the increase of shear stiffness, displacement is more distributed along the reinforcement, while for decrease of shear stiffness the displacement is more localized. But the effect of subgrade stiffness on the displacement profile is quite opposite compared to the effect of shear stiffness. At higher values of subgrade stiffness, the displacements are localized at the pulling end and the displacements progress towards the far end for lower values of subgrade stiffness. Higher the obliquity of pull, steeper the deformation profile. The displacement at any point in the reinforcement decreases with the increase in shear stiffness but increases with increase in obliquity. With increase in shear stiffness, soil shares more load by distributing the load over larger area. As a result, normal stresses developed in the soil reinforcement interface reduce and hence resulting in decrease in interface shearing resistance.. Hence, displacement at end and tension generated in the reinforcement decreases. Inclination of the reinforcement force is more at the pulling end and becomes horizontal at the far end. The direction of the tensile force at the pulling end is more or less horizontal for higher values of shear stiffness. With the decrease of shear stiffness, inclination of the tensile force in the reinforcement increases and becomes equal to the inclination of the applied force. For higher values of subgrade stiffness, change in the direction of the tensile force along the reinforcement is more due to localized deformation of the reinforcement. The direction of the reinforcement force increases with the increase in obliquity of the pullout force [27].

Patra and Shahu (2012) presented an analysis on the evaluation of the pullout capacity of sheet reinforcement subjected to oblique pullout force considering soil subgrade as a two parameter linear elastic Pasternak model and the reinforcement as inextensible. An

inextensible sheet reinforcement of length l embedded at depth D is resting on a subgrade soil. The reinforcement is subjected to an oblique force P at a point B where the sliding mass intersects the reinforcement.

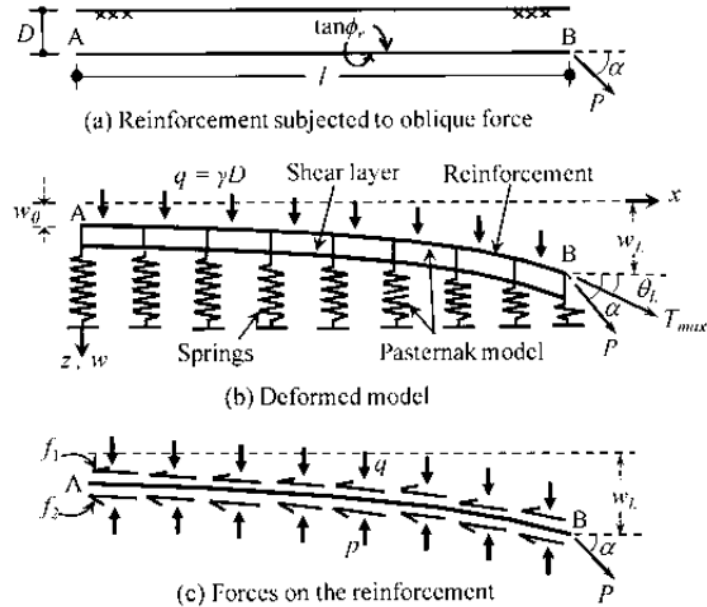


Figure 2.5: Schematic of the model used [19]

Use of Pasternak model made the oblique pull out analysis more realistic. It was found that the orientation of the reinforcement at the pull out end is different from the direction of the pullout force and depends on the shear modulus of the subgrade soil. Oblique pull out test results were compared with direct measurement of the reinforcement inclination in the vicinity of the failure surface. Under the action of oblique pull, the reinforcement undergoes transverse deformation and the soil beneath the reinforcement mobilizes additional normal and shear stresses thus increasing the pull out capacity of the reinforcement [19].

Krunoslav and Mensur (2013) presented a review of soil and reinforcement interaction testing in reinforced soil by pull out test. It was observed that at high values of normal stresses and/or large reinforcement length, the reinforcement failure mainly occurs due to tensile failure instead of pullout. Increase of soil compaction and density increases the possibility of interlocking of soil particles in the grid apertures which increases the pull out resistance. Higher compaction can cause tensile failure of reinforcement [25]. Pull out force increases with increase in the soil grain diameter. Pull out resistance significantly depends on the S/D_{50} ratio (S is the size of geogrid apertures expressed as

the distance between grid transversal ribs and D_{50} is the average soil grain size). The study results show that for medium to fine silica sand with $D_{50}=0.6$ mm and aperture opening of 30 – 100 mm, maximum pull out resistance is achieved at $S/D_{50} = 50$. Similar observations were found for $S/D_{50}>3$. Reinforcement influence extends approximately to the distance of $30D_{50}$ measured vertically from the geogrid plane [26].

Chapter 3

Materials Properties

3.1 Introduction

This Chapter presents the characteristics of materials (sand and reinforcements) used in the research work. Various tests performed on sand and reinforcement along with the test results are presented.

3.2 Characteristics of Sand

The sand used in the research work was obtained from Vijayawada. When procured, it was slightly moist. To remove the moisture, it was air-dried for one week by spreading in thin layers over polythene sheets. Gravel particles were removed by sieving the sample through 4.75 mm sieve.

3.2.1 Sieve Analysis

To know the particle size distribution, sieve analysis was conducted on sand as per IS: 2386 (Part I)-1963. Based on the sieve analysis, the size of the sand particles was found to range from 0.15 mm to 1.18 mm. The effective size or effective diameter (D_{10}) of the sample is 0.33 mm and average grain size of the particle (D_{50}) is 0.8 mm. The Coefficient of Uniformity, C_u , and the Coefficient of Curvature, C_c , were found to be equal to 2.63 and 1.01, respectively. As per Indian standard Classification System (ISCS) (IS: 1498-1970) [13], sand is classified as Poorly Graded (SP).

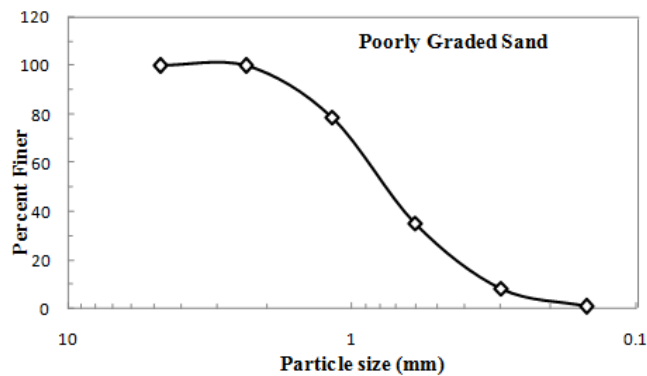


Figure 3.1: Gradation Analysis.

3.2.2 Specific gravity

Specific gravity test was conducted as per IS: 2720 (Part III/Sec 1) – 1980 [8] and a specific gravity value, G_s , equal to 2.71 was obtained.

3.2.3 Maximum and minimum dry densities

The maximum dry density [9] and minimum dry density [21] of the sample are found to be 16.8 kN/m^3 and 14.8 kN/m^3 , respectively. Based on these density values and G_s value, the maximum and minimum void ratios of sand were calculated and found to be equal to 0.79 and 0.56, respectively.

3.2.4 Direct Shear Test

To find the shear strength parameters of test sand, automated Large-scale direct shear apparatus is used. Tests are conducted as per IS 2720 (Part XXXIX/Sec. I) [10]. The box has inner dimensions of 300 mm x 300 mm x 200 mm (Figure 3.2). Apparatus consists of horizontal and vertical loads cells with maximum capacity of 44 kN each. The maximum allowable horizontal displacement of the lower box is 50 mm. During the shearing process, the horizontal displacement of the lower box and vertical displacement of the soil sample using horizontal and vertical linear variable differential transformers (LVDTs) . This set-up uses a closed-feedback system from transducers to provide real-time control of the load frame. Two force transducers (horizontal and vertical) and two displacement transducers (horizontal and vertical) are used. The computer loads or unloads the sample in the box until the readings from the transducers equal the values required to meet the test specifications. The loading mechanism to apply normal load is raised and lowered by a micro – stepper motor that is connected to a worm gear. The loading mechanism to apply shear loads is moved left and right by a second combination of micro-stepper motor and worm gear. Limit switches for both

horizontal and vertical motions prevent running the loading mechanism beyond its physical limits. Sand sample in the shear box is prepared by using the compaction technique. Details of the compactor used are discussed in Chapter 4 (Section 4.3). Sand sample is compacted in two layers of thickness 100 mm. Four blows are given on each layer. Dry density of sand achieved is 16.1 kN/m^3 . This corresponds to a sample of relative density equal to 67%.

Tests are conducted at three different normal stresses of 50 kPa, 100 kPa and 150 kPa. The rate of displacement of lower box is 1 mm/minute. Shear stress values are recorded at every 1 mm horizontal displacement of the lower box. Graphs are drawn showing the variation of shear stress and horizontal displacement for three normal stresses (Figure 3.3).

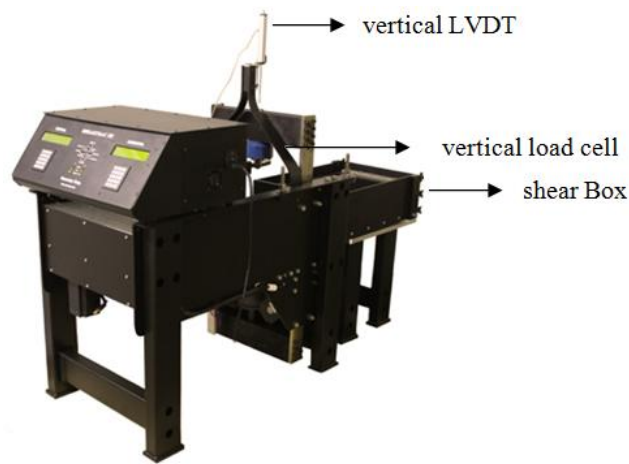


Figure 3.2: Large Scale Direct Shear Apparatus

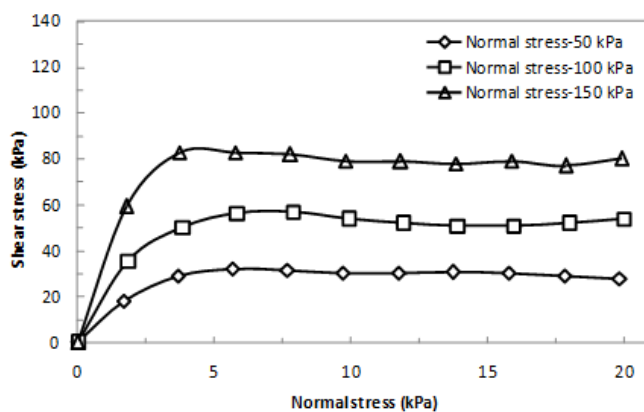


Figure 3.3: Shear stress vs. Horizontal displacement

The values of maximum shear stress (from Figure 3.3) are plotted against the normal stress to obtain the shear strength envelope.

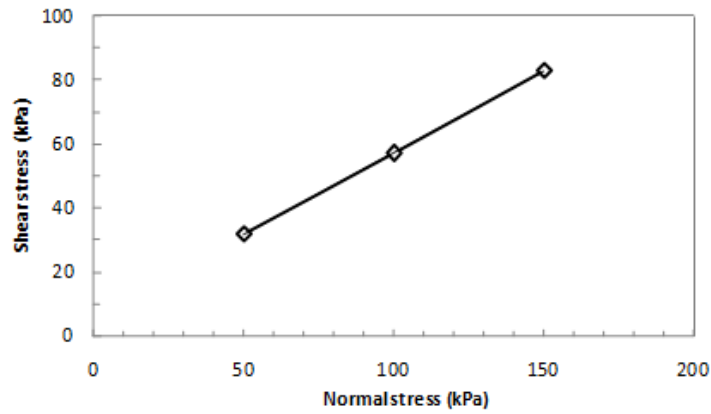


Figure 3.4: Normal Stress vs. Maximum shear Stress

From Figure 3.4, the apparent cohesion and the end-of-test angle of shearing resistance of sand are found to be 0.1 kPa and 29° , respectively.

3.3 Reinforcement Characteristics

Two types of reinforcements are considered in the study- Geogrid and Strip.

3.3.1 Geogrid

Geogrid Reinforcement is made of stretched monolithic white polypropylene flat bars with welded junctions. Table 3.1 gives the important properties of the geogrid used. This geogrid was manufactured by Secugrid. Photographic view of the geogrid used for the test is shown below.

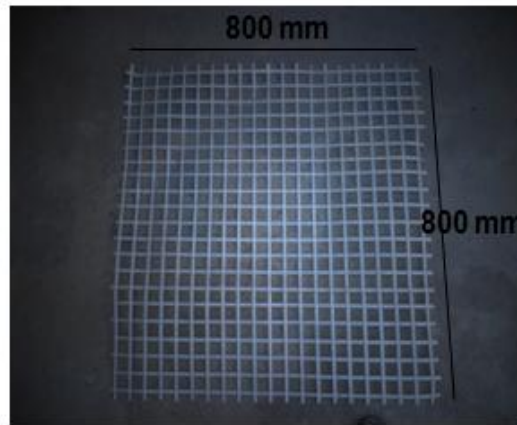


Figure 3.7: Geogrid used in the test

Table 3.1: Properties of Geogrid

| Property | Test method | Units | Value |
|---------------|-------------|-------|---------------------------|
| Raw materials | - | - | Polypropylene (PP), White |

| | | | |
|-----------------------------------|-------------------------|------------------|-----------------|
| Mass per unit area | EN ISO 9864 (EN 965) | g/m ² | 240 |
| Max. Tensile strength | EN ISO 10319 | kN/m | 40 |
| Elongation at nominal strength | EN ISO 10319 | % | 8 |
| Tensile strength at 2% elongation | EN ISO 10319 | kN/m | 16 |
| Tensile strength at 5% elongation | EN ISO 10319 | kN/m | 32 |
| Aperture size | - | mm | Approx. 31 x 31 |
| Rib thickness | - | Mm | 0.85 |

3.3.2 Paraweb Strip

Paraweb strips are planar structure consisting of a core of high tenacity polyester yarn tendons encased in a polyethylene sheath. These have several advantages, namely, high standard tensile strength up to 135 kN, high modulus, high toughness and durable polyethylene sheath, low creep characteristics, easy to install, high resistant to chemicals, micro-organisms, UV radiation and mechanical damage. For the present study, Paraweb strips of tensile strength 100 kN are used [12]. Photographic view of the strip used for the test is shown below.



Figure 3.8: Strip used in the test

Table 3.1: Properties of Strip

| Property | Unit | Value |
|-----------|------|-------|
| Width | mm | 88.5 |
| Length | mm | 765 |
| Thickness | mm | 2.05 |

| | | |
|-----------------------|----------------|------|
| Mass per unit area | g/m^2 | 1020 |
| Max. Tensile strength | kN/m | 100 |

3.4 Interface Direct Shear Test

Interface direct shear test is conducted using large scale direct shear apparatus [14]. Test procedure is similar direct shear test discussed in Section 3.2.3 with the only difference that geogrid is introduced at the interface of two boxes. After filling the lower box through compaction technique, geogrid of size 200 mm wide and 400 mm long is firmly attached to the lower box. The geogrid properties are given in Section 3.3 below. The upper box is then placed over the lower box and sand is filled in the upper box and compacted. The sample is subjected to shear at three different normal stresses to obtain interface shear strength properties.

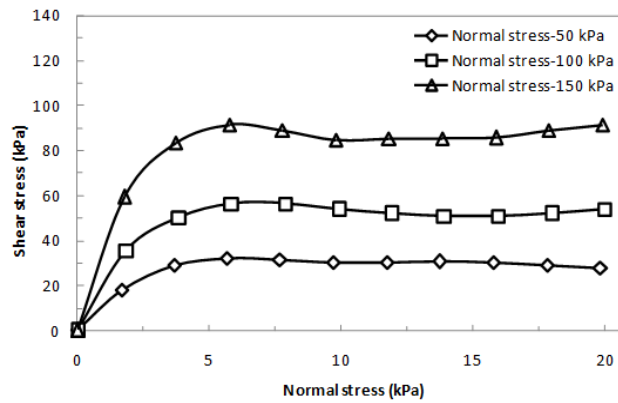


Figure 3.5: Shear stress vs. horizontal displacement for geogrid interface

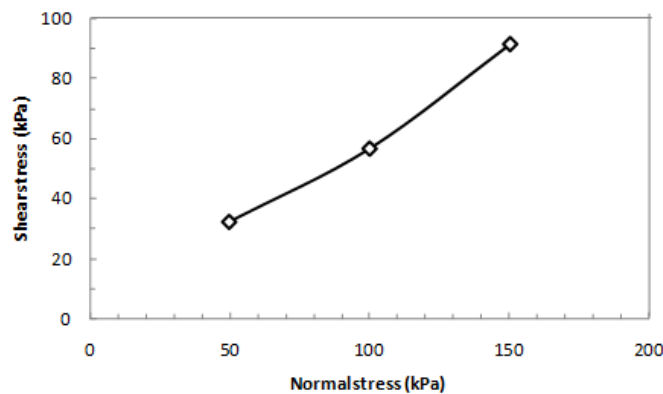


Figure 3.6: Normal stress vs. shear stress for geogrid interface

From Figure 3.6, the apparent cohesion and angle of shearing resistance of sand are found to be 0.865 kPa and 30° respectively. Consequently, there is an increase in the angle of shearing resistance by 11% with the use of geogrid at the interface.

Chapter 4

Test Methodology

4.1 Introduction

This chapter consists of three sections. In the first section, the details of test setup used for the study are presented. It explains the shear box that is specially fabricated for testing to conduct the testing, the arrangement and position of gauges, etc. Numerous photographs are showed for its better understanding. In the second section, details on sample preparation are presented. It includes details on the shear box and for preparing sand beds of required and uniform relative density and on procedure that is followed for preparing unreinforced and reinforced sand beds, etc. In the third section, test procedure is presented.

4.2 Test Setup

The apparatus used for testing is a new pattern of direct shear apparatus through which soil can be sheared in a vertical plane. It consists of large size shear box along with accessories such as springs, dial gauges with magnetic stand, hydraulic jacks with proving rings, etc.

4.2.1 Shear Box

A metallic shear box is used for testing. It has the dimensions of 1000 mm (length) x 1000 mm (width) x 600 mm (height). The thickness of the walls of the box is equal to 5 mm. Box is open at its top whereas at its base, right half is fixed and left half open (Figure 4.1). It consists of two top plates of dimension 1000 mm x 500 mm x 5 mm

used to apply load on the prepared sand samples. These plates are provided with handles to enable lifting and placement on the prepared sand samples.

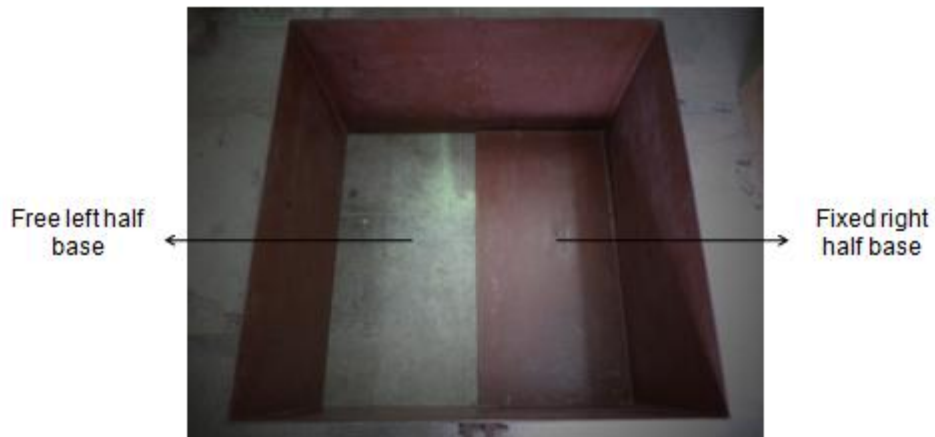


Figure 4.1: Top view of unfilled shear box.

The walls of the box are painted on both inside and outside surfaces to prevent corrosion and also to provide smooth surface to reduce friction while loading is under process. The base of right half of the box rests on solid support (concrete bricks) as shown in Figure 4.2.



Figure 4.2: Front view of shear box.

Beneath the left-half base of the box, springs are placed such that top level of the springs is 50 mm above the right-half base (Figure 4.3). The arrangement of springs beneath left-half base plate is shown in Figure 4.4.

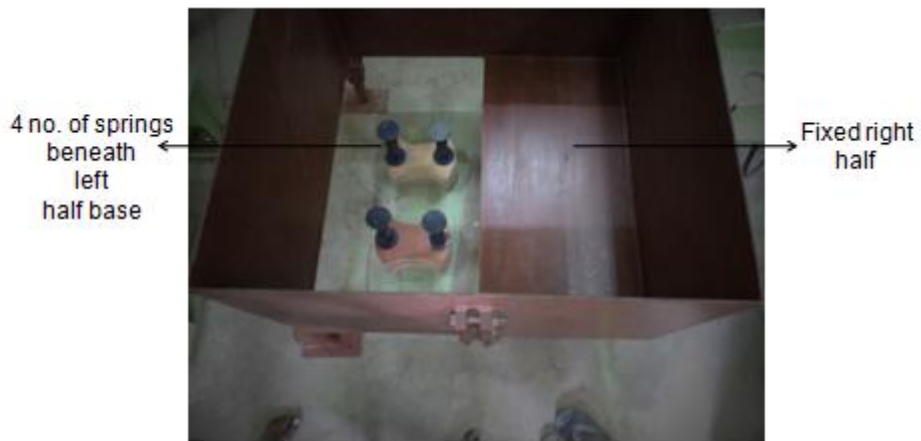


Figure 4.3: Springs below left half base.

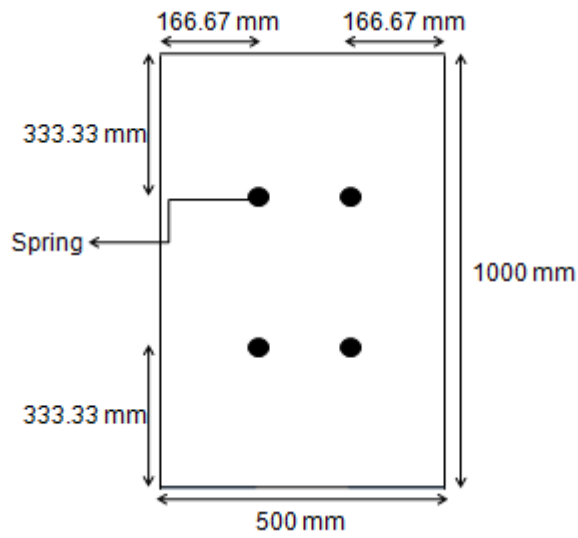


Figure 4.4. Arrangement of springs beneath left-half base plate

Movable left half base plate is placed over the springs and checked for level using spirit level (Figure 4.5).



Figure 4.5: Check for levelling of left-half base plate.

The gap between two base plates at different level is bridged using a wooden plank of dimension 1000 mm x 100 mm x 20 mm (Figure 4.6)



Figure 4.6: Base plates bridged with a wooden beam.

The inner walls of the box are lubricated using a lubricant (grease) and a polythene sheet is placed over the applied lubricant layer to reduce the friction between sand sample and the walls of the box (Figure 4.7).



Figure 4.7: Inside of shear box covered with polythene sheet.

Dial gauges are attached beneath the movable left base plate near its four corners to measure the displacement of movable plate under applied load (Figure 4.8). Sand is filled in the shear box in a specific manner (as detailed in section 4.3) and leveled (Figure 4.9). Two top plates are placed over the prepared sand beds in the shear box (Figure 4.10). Hydraulic jacks with proving ring are placed on left and right top plates at

their centre for applying load in increments. Hydraulic jacks are rested against a rigid metal plate of reaction frame to get reaction (Figure 4.11).

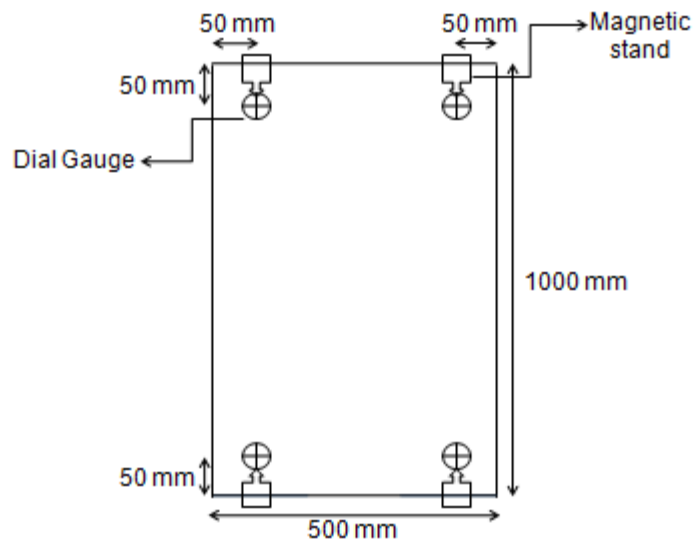


Figure 4.8: Arrangement of dial gauges beneath left base plate



Figure 4.9: Levelling of prepared sample



Figure 4.10: Placing of top plates



Figure 4.11: Front view of shear test apparatus

4.2.2 Springs

Four numbers of springs are used in the test. Springs are provided with cap of diameter 50 mm at top and bottom so that they can provide large bearing area for movable plate resting on them and get large supporting area from ground on which they are resting (Figure 4.12).



Figure 4.12: Spring

Load vs. Settlement curve for group of four spring assembly is shown in Figure 4.13.

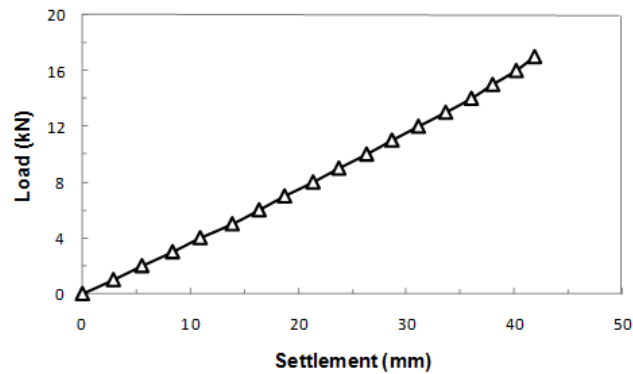


Figure 4.13: Load vs. Settlement graph for spring assembly

From the above curve, stiffness (load/settlement) of the spring assembly is found to be 0.399 kN/mm. Springs can undergo maximum settlement of 40 mm.

4.2.3 Dial Gauges

Four number of dial gauges (Figure 4.14) are used during testing. Dial gauges are provided with magnetic stands so that it can be easily attached with the shear box in required position. Least count of the dial gauges is 0.01 mm.



Figure 4.14: Dial gauge with magnetic stand

4.2.4 Hydraulic Jacks with Proving ring.

Load on the sand sample is applied through two hydraulic Jacks. Maximum rated capacity of each hydraulic Jack is 50 kN. Proving ring is connected with hydraulic Jack to measure the applied load (Figure 4.15). Load applied vs. Proving ring reading is shown in Figure 4.16. A metallic circular plate of 100 mm diameter and 25 mm

thickness is connected at the top of both proving ring to have large bearing area against reaction plate.



Figure 4.15: Hydraulic Jack with Proving ring

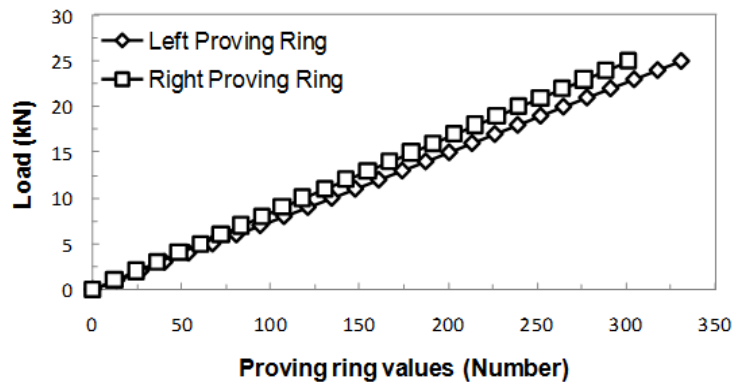


Figure 4.16: Load vs. Proving ring reading

4.3 Sample Preparation

Sand beds of required and uniform relative density are prepared in the shear box by using a compaction technique.

4.3.1 Compactor

The compactor used for the purpose is shown in Figure 4.17.

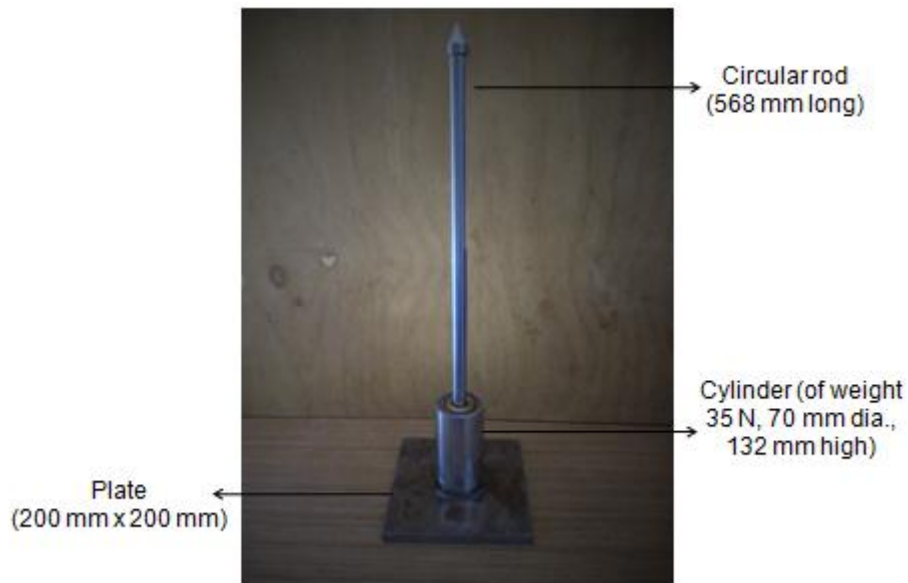


Figure 4.17: Compactor

The compactor has steel base plate of dimension 200 mm x 200 mm x 12.5 mm. A steel rod of length 568 mm is attached to the base plate. A steel cylinder of height 132 mm, diameter 70 mm and weight 35 N is made to fall on base plate from a height of 436 mm by guiding over steel rod. Total depth of sample prepared is 400 mm. It is prepared in four layers each of thickness 100 mm. 50 number of blows are uniformly applied on each layer with the compactor (Figure 4.18).



Figure 4.18: Compaction of sand layers.

Compacting energy imparted on each layer ($35 \text{ N (weight)} \times 0.436 \text{ m (height of fall)} \times 50 \text{ (no. of blows)}$) is 763 N-m. To determine the density of sand achieved after compaction, weight of sand poured in each layer is measured. The thickness of each layer is obtained by measuring the levels of sand from the top of box before and after

compacting the layer. Eight readings were taken along the sides of the box to get a representative value of the level of sand measured from the top. The difference between two depths gives the thickness of compacted sand in a layer at various points. Average depth of the compacted sand multiplied by area of box gives the volume of sand in a layer. The weight of the sand poured divided by its compacted volume give the density achieved. The density achieved through present compacting effort is 16.08 kN/m^3 . With the maximum and minimum density of sand known, Relative density of the sample is calculated using the expression below.

$$\text{Relative Density} = \frac{\gamma_{dmax} (\gamma_d - \gamma_{dmin})}{\gamma_d (\gamma_{dmax} - \gamma_{dmin})} \dots \dots \dots (4.1)$$

Where, γ_{dmax} = Maximum dry density of sand = 16.8 kN/m^3 .

γ_{dmin} = Minimum dry density of sand = 14.8 kN/m^3 .

γ_d = Density achieved in shear box = 16.08 kN/m^3 .

4.3.2 Geogrid Reinforced Sand

In case of geogrid reinforced sand, the first layer of compacted sand is prepared and the geogrid (800 mm x 800 mm in plan dimensions) is paced on the compacted layer Geogrid is placed such that a uniform spacing of 100 mm is maintained between all around geogrid and walls of the shear box (Figure 4.19). The process of placing and compacting sand layer and placing geogrid on it is continued for two more layers. The fourth layer of sample is placed over third layer of geogrid and compacted.

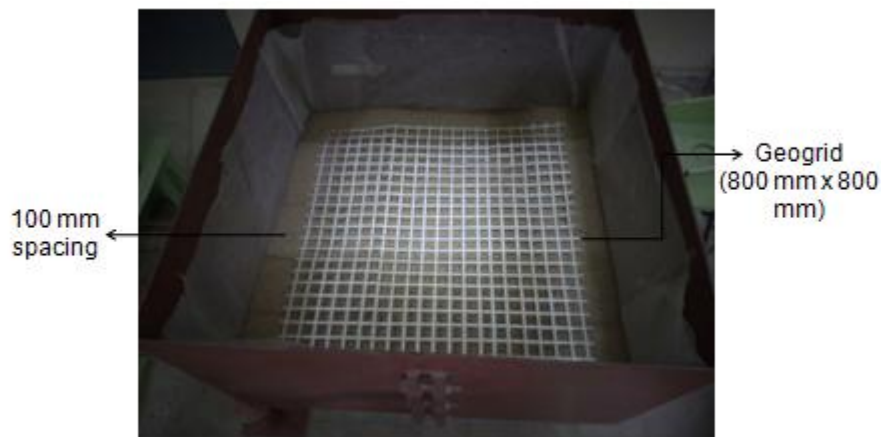


Figure 4.19: Placement of Geogrid

4.3.3 Paraweb Strips Reinforced Sand

In case of Paraweb strips reinforced sand, the first layer of compacted sand is prepared. Over it, Paraweb strip of length 765 mm is placed such that a spacing of 100 mm is maintained between outermost strips and sides of shear box. Clear spacing between two successive strips in a layer is 148.6 mm (Figure 4.20). Over it second layer of sample is placed and compacted. This process is repeated until fourth layer of sample is placed over third layer of strips and compacted.



Figure 4.20: Placement of Paraweb Strips

4.4 Test Procedure

Step by step procedure followed while performing the test is discussed below.

- Apply a given normal load (equal to 10 kN/20 kN/30 kN) with the hydraulic jack on the right half top plate of the shear box.
- Due to the application of vertical load of normal load on the right half top plate, normal stresses are developed over middle vertical section of the sand sample which is calculated using a commercially available Finite element software - Plaxis 3D.
- Note down the initial reading of all the four dial gauges attached beneath the left half base plate of the shear box.
- Apply the load on left half top plate of the shear box with the hydraulic jack at a rate of 1 kN/minute.
- Load is applied at an increment of 1 kN.
- After every incremental value of load applied, note down the reading of all the four dial gauges to know the displacement of soil in the vertical plane under applied load.

- To know the shear stress acting over vertical shear plane at every increment of load applied, following equilibrium equation is used.

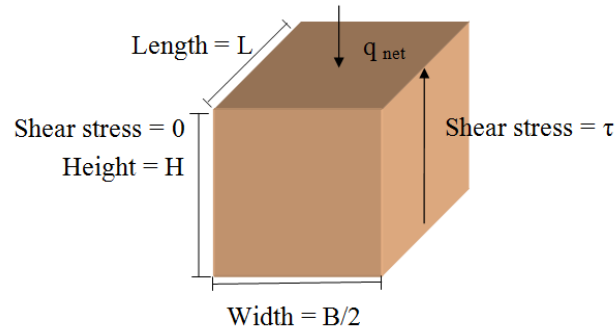


Figure 4.21: Left half soil mass in shear box.

q_{net} = Cumulative load applied – Spring stiffness x corresponding cumulative settlement

For equilibrium of left half soil mass

$$\tau \times H \times L = q_{net} \times B/2 \times L$$

$$\tau = q_{net} / 2 \times H \quad (\text{as } B = 1 \text{ m and } H = 1 \text{ m})$$

where,

τ = Shear stress in kPa acting over middle vertical cross section of sand sample in shear box.

q_{net} = Net vertical stress in kPa acting on left soil mass in shear box.

L = Length of shear box ($L = 1 \text{ m}$)

B = Width of shear box ($B = 1 \text{ m}$)

H = Height of sample prepared ($H = 400 \text{ mm}$)

- With the known values of shear stress at every load increment and corresponding shear displacement, a plot between shear stress and shear displacement in vertical plane is drawn.
- Test is conducted for three different vertical loads 10 kN, 15 kN and 20 kN on right half top plate.
- Similar procedure is followed for sand reinforced with geogrid and strips. Improvement in the shear strength of reinforced sand (with three layers of reinforcement) over unreinforced sand is reported.

Chapter 5

Results and Conclusions

5.1 Introduction

Introduction of reinforcement in sand increases the stiffness and shear strength parameters of sand that results in increasing its stability. In this Chapter, increase in the shear strength parameters of sand reinforced with geogrids and strips are discussed.

5.2 Unreinforced Sand

Unreinforced sand is subjected to shear along vertical plane with three different normal loads of 10 kN, 15 kN and 20 kN applied over right half of the top-plate of the large shear box. Shear stress along the vertical plane vs. vertical displacement of left half of the box obtained for three loads are shown in Figure 5.1.

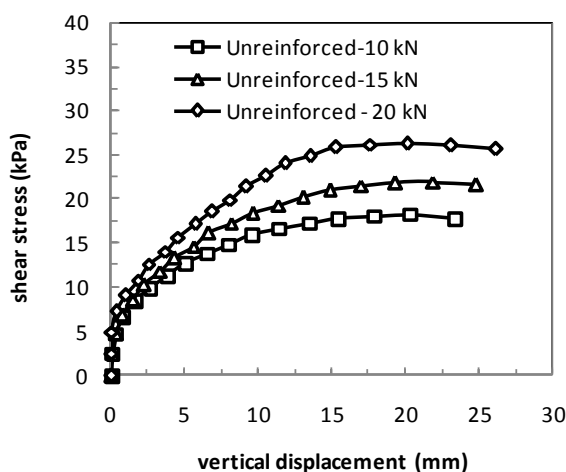


Figure 5.1: Shear stress along vertical plane vs. vertical displacement of bottom of left-half of the box for unreinforced sand

Horizontal stresses acting over vertical shearing plane due to the application of normal load over the top of right half of the shear box is calculated using Finite element based software -Plaxis 3D. The models created in Plaxis 3D for different loading conditions

with fine mesh are shown below (Figure 5.2 to 5.5). In the initial loading condition, normal load on the right top alone is considered and the normal stress developed over vertical shearing plane is determined. In the failure condition, normal load over right top plate along with normal load over left top plate corresponding to failure condition are considered and consequent horizontal stress developed over shearing plane is determined.

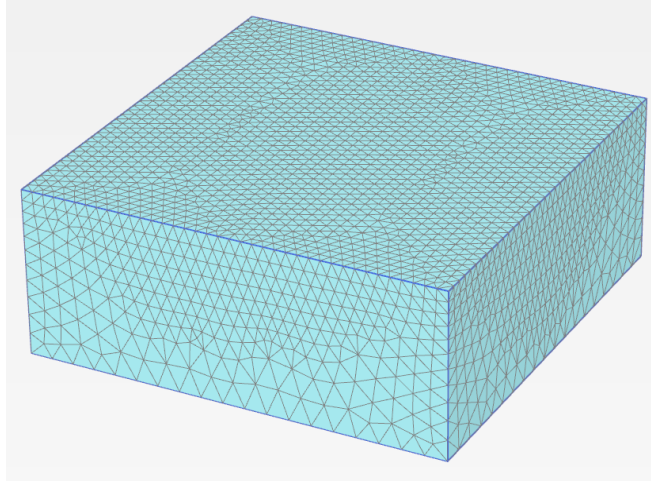


Figure 5.2: Test soil mass model in Plaxis

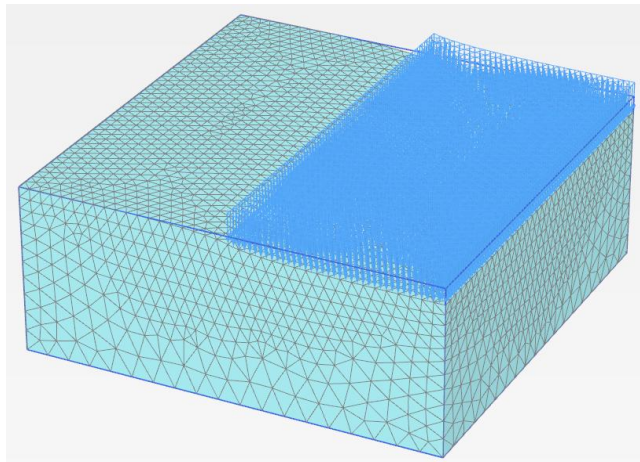


Figure 5.3: Model of test soil mass at initial condition

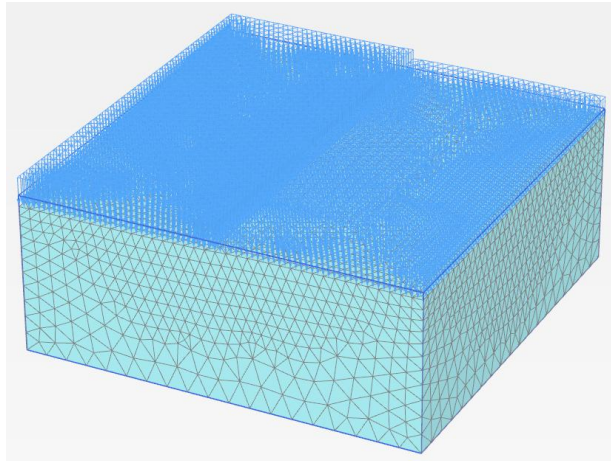


Figure 5.4: Model of test soil mass at failure condition

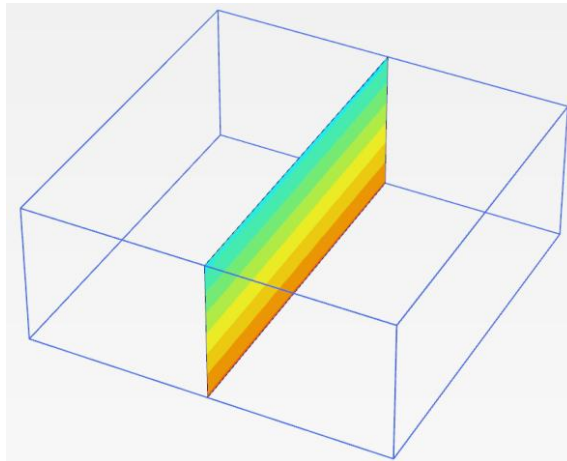


Figure 5.5: Normal stress contours along the shearing plane in test soil mass model

The model in Plaxis 3D is created with the parameters listed in Table 5.1.

Table 5.1: Parameters used in Plaxis 3D

| Parameter | Value |
|---------------------|------------------------|
| Material model | Linear elastic |
| Unit weight of sand | 16.1 kN/m ³ |
| Elastic modulus | 1600 kPa |
| Poisson's ratio | 0.3 |

Table below shows the failure shear stresses and horizontal stresses developed over shearing plane under initial and failure condition. It may be noted that the horizontal stresses correspond to the normal stresses on the shearing plane.

Table 5.2: Horizontal stresses over shearing plane

| Normal load on right top plate (kN) | Shear stress at failure (kPa) | Horizontal stress over shearing plane (kPa) | |
|--|----------------------------------|--|----------------------|
| | | Initial condition | Failure condition |
| 10 | 18.2 | 7.39 | 13.4 |
| 15 | 21.9 | 9.33 | 15.8 |
| 20 | 26.3 | 11.21 | 20.0 |

Graph between failure shear stress values (obtained from Figure 5.1) and horizontal stress values at failure (shown in Table 5.1) is drawn to obtain the shear strength parameters along vertical plane for unreinforced sand as shown in Figure 5.6.

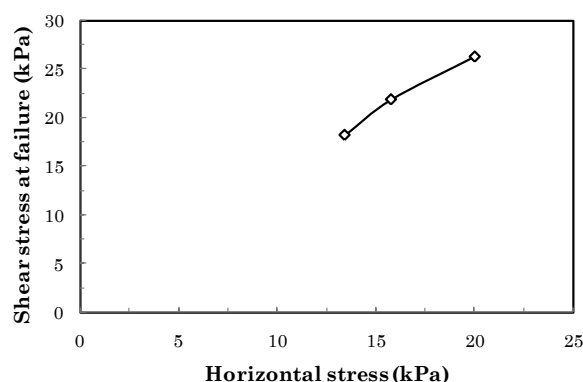


Figure 5.6: Shear stress vs. horizontal stress at failure

From the shear strength envelope shown in Figure 5.6, the angle of shearing resistance of sand for shearing along vertical plane is found to be 50° .

The high value of angle of shearing resistance of sand observed in above case is due to low normal stresses acting over shearing plane which is justified by conducting the conventional large-scale direct shear test [10] at normal stresses corresponding to failure condition in shear tests along vertical plane. Figure 5.7 shows the shear stress vs. horizontal displacement curves for samples prepared with the same relative density when subjected to normal stresses corresponding to values given in Table 5.1.

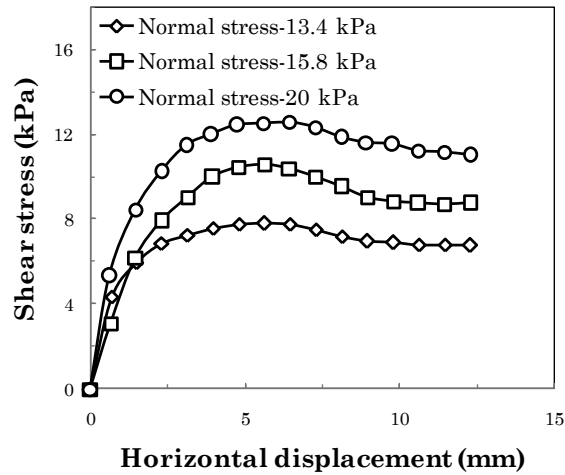


Figure 5.7: Shear stress vs. horizontal displacement from conventional direct shear testing (shearing along horizontal plane)

The angle of shearing resistance of sand is obtained as 48° corresponding to the maximum shear stresses from Figure 5.7 and corresponding horizontal stresses.

5.3 Reinforced Sand

Shear stress vs. vertical displacement curves for geogrid reinforced sand for three different normal loads on right top plate is shown in Figure 5.8. It may be noted that three layers of geogrid are used in the testing.

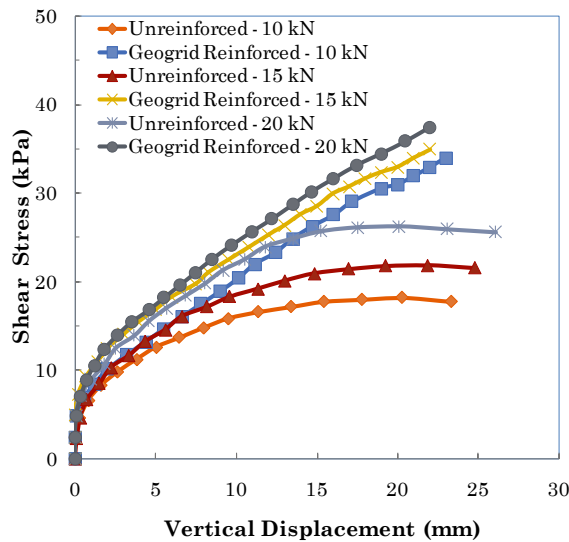


Figure 5.8: Shear stress vs. vertical displacement for geogrid reinforced sand

From Figure 5.8, it can be observed that the geogrid reinforced sand initially follows the trend of unreinforced sand. This can be because up to the displacement corresponding to 5 kPa shear stress, tensile force in the reinforcement is not mobilized. For higher stress

values, geogrid reinforced sand curves shows the continuously raising shear stress vs. vertical displacement behavior. The mobilized angle of shearing resistance at 20 mm displacement is 63° .

Shear stress vs. vertical displacement curves for strips reinforced sand for three different normal loads on right top plate is shown in Figure 5.9.

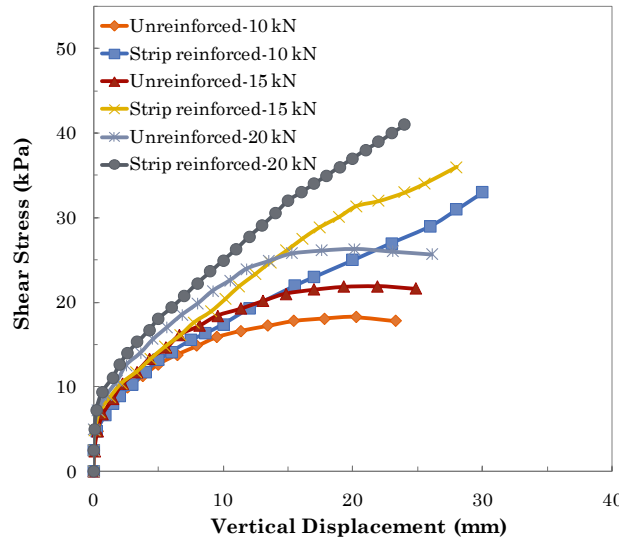


Figure 5.9: Shear stress vs. vertical displacement for Strips reinforced sand

From Figure 5.9, it can be observed that strips reinforced sand curve follows the trend of unreinforced sand up to 6.5 kPa shear stress and for higher stresses, strips reinforced sand curves shows the continuously increasing improvement in the behavior compared to that for unreinforced case. The mobilized angle of shearing resistance at 20 mm displacement is 62° .

The failure stress can be obtained by assuming that the shear stress bears a hyperbolic relationship with the displacement. This relationship can be given by

$$\tau = \frac{k_{\tau} \delta}{1 + \frac{k_{\tau} \delta}{\tau_{ult}}} \dots\dots(5.1)$$

On rearranging the terms, we obtain

$$\frac{\delta}{\tau} = \frac{1}{k_z} + \frac{1}{\tau_{ult}} \delta \dots\dots(5.2)$$

where,

δ = Vertical displacement (mm).

τ = Shear stress (at displacement δ) (kPa).

$1/k_z$ = Intercept of curve on vertical axis (kPa)

τ_{ult} = Ultimate shear stress (kPa)

The graph is drawn between δ/τ and δ for the linear variation of shear stress vs. vertical displacement (for the displacement between 5 mm 25 mm) as shown below. The inverse of the slope of fitted lines is taken as the failure shear stress.

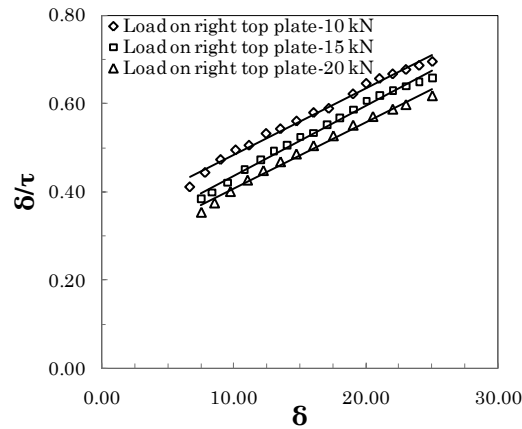


Figure 5.10: δ/τ vs. δ for Geogrid reinforced sand

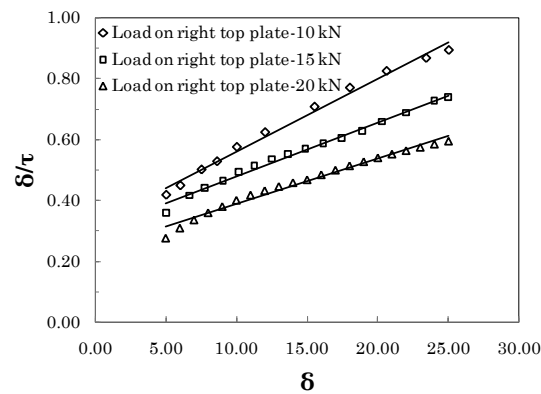


Figure 5.11: δ/τ vs. δ for Strips reinforced sand

The failure shear stress values obtained from Figures 5.10 and 5.11 for geogrid and strip reinforced sand respectively, using equation 5.1 is shown in Table 5.3.

Table 5.3: Failure shear stress for Reinforced sand

| Normal load on right top plate (kN) | Horizontal stress on shearing plane (kPa) | Failure shear stress for geogrid reinforced sand (kPa) | Failure shear stress for strip reinforced sand (kPa) |
|---|--|---|---|
| 10 | 13.4 | 6.5 | 50 |
| 15 | 15.8 | 66.5 | 62 |
| 20 | 20.0 | 70.5 | 74 |

5.4 Conclusions

- ❖ A new pattern of shear apparatus is designed to find the shear strength parameters of sand along vertical plane.
- ❖ The angle of shearing resistance of sand along vertical plane obtained from new pattern of shear apparatus is almost same as the one obtained along horizontal plane using conventional large-scale direct shear apparatus.
- ❖ Improvement in reinforced sand over unreinforced sand is compared.

Table 5.4: Improvement in angle of shearing resistance of reinforced sand over unreinforced sand

| Type of sample | Angle of shearing resistance (ϕ) Corresponding to failure shear stress | % Increase in $\tan(\phi)$ over unreinforced sand |
|-------------------------|--|---|
| Unreinforced | 50° | - |
| Geogrid reinforced sand | 76° | 236 |
| Strips reinforced sand | 75° | 213 |

References

- [1] “Some Observations of Geotechnical Aspects of the February 28, 2001, Nisqually Earthquake in Olympia, South Seattle, and Tacoma, Washington”. Pacific Earthquake Engineering Research Center.
- [2] Polemio. M and Lollino. P.(2011) Failure of Earthen embankments induced by flooding and seepage: a neglected source of hazard. Copernicus publications on behalf of the European geosciences union.
- [3] “Construction Materials for Civil Engineering” by Errol Van Amsterdam
- [4] Jewell, R.A. (1996) Soil Reinforcement with Geotextiles, Construction Industry Research and Information Association (CIRIA) Special Publication 123.
- [5] Jewell. R.A. and Wroth, C.P. (1987). Direct shear tests on reinforced sand, Geotechnique, vol. 37, No. 1, pp 53 – 68.
- [6] Umashankar. B, Hari Prasad. C and Madhav M.R (2012). Modeling Reinforcement-Soil Interactions under Oblique or Transverse Forces- A Review. Proceedings of asiafuge.
- [7] IS 1498 : 1970 Classification and identification of soils for general engineering purposes.
- [8] IS: 2720 (Part III/Sec 1) – 1980 Specific gravity of fine-grained soil by density bottle method.
- [9] ASTM D 4253 - 00(2006): Standard Test Methods for Maximum Index Density and Unit Weight of Soils Using a Vibratory Table.
- [10] IS 2720 (Part XXXIX/Sec. I): Large Direct Apparatus.
- [11] ASTM D 4595-86 (2001): Standard Method for Tensile Properties of Geotextile by Wide Width Strip Method.
- [12] ASTM D 6637-11: Standard Test Method for Determining Tensile Properties of Geogrids by the Single or Multi-Rib Tensile Method.
- [13] IS: 1498-1970 Indian Standard Classification And Identification Of Soils For General Engineering Purposes.
- [14] ASTM D5321 - 12 Standard Test Method for Determining the Shear Strength of Soil-Geosynthetic and Geosynthetic-Geosynthetic Interfaces by Direct Shear.

- [15] Bergado. D. T, Teerawattanasuk and Long. P. V (2000). Localized mobilization of reinforcement force and its direction at the vicinity of failure surface. *Geotextile and Geomembranes* 18 (2000) 311-331.
- [16] Madhav, M.R., and Umashankar, B. (2003a) “Analysis of Inextensible Sheet Reinforcement Subject to Transverse Displacement/Force: Linear Subgrade response”, *Geotextiles and Geomembranes*, Vol. 21, No. 1, pp. 69-84.
- [17] B. Umashankar, C. Hari Prasad and M. R.Madhav (2012).” Modeling Reinforcement-Soil Interactions under Oblique or Transverse Forces- A Review”. *Proceeding of Asiafuge*.
- [18] Binod Shrestha and Hadi Khabbaz (2010).” Improving Reinforced Soil Performance Incorporating Vertical Reinforcement”. *Geoshanghai International Conference*.
- [19] Patra, S. and Shahu, J. (2012). ”Pasternak Model for Oblique Pullout of Inextensible Reinforcement.” *J. Geotech. Geoenviron. Eng.*, 138(12), 1503–1513.
- [20] Madhav, M. R., and Umashankar, B. (2003b). “Analysis of Inextensible Sheet Reinforcement subject to Downward Displacement / Force: Nonlinear Subgrade Response”, *Geosynthetics International*, Vol. 10, No. 3, pp. 95-102.
- [21] ASTM D 4254 – Standard Test Methods for Minimum Index Density and Unit Weight of Soils and Calculation of Relative Density.
- [22] Alfaro, M.C., Hayashi, s., Miura, N. and Watanabe, K., (1995), “Pullout Interaction Mechanism of Geogrid Strip Reinforcement”, *Geosynthetics International*, Vol. 2, No. 4, pp. 679-698.
- [23] Schlosser, F. and Elias, V., 1978, “ Friction in Reinforced Earth”, *Proceedings of the ASCE Symposium on Earth Reinforcement*, ASCE, Pittsburgh, PA, USA, April 1978, pp. 735-763.
- [24] Shahu. J.T. (2007). “ Pullout resistance of Inextensible sheet reinforcement subject to oblique end force”. *Journal of Geotechnical and Geoenvironmental Engineering*, Vol. 133, ASCE
- [25] Sieira, A.C.C.F (2003): *Experimental study on Soil-Geogrid interaction mechanism*, PhD Thesis, Pontifical University of Rio de Janeiro, Brazil, 377p.
- [26] Krunoslav Mizanek and Mensur Mulabdic (2013). “ A Review of soil and reinforcement interaction testing in reinforced soil by pullout test”. *Gradevinar* 65.
- [27] Shantanu Patra Shahu. J. T. (2011). “Effect of subgrade stiffness on oblique pullout behavior of reinforced soil”. *Proceedings of Indian Geotechnical Conference*, December 15-17, 2011, Kochi.

- [28] Chia-Nan Liu, Jorge G. Zornberg, Tsong-Chia Chen, Yu-Hsien Ho and Bo-Hung Lin. (2009). "Behavior of Geogrid-Sand interface in Direct shear mode". Journal of Geotechnical and Geoenvironmental Engineering, ASCE.
- [29] Palmeira, E.M. "Soil-Geosynthetic interaction: Modeling and Analysis (Mercer lecture 2007-2008), Proceeding of the 4th European Geosynthetics Conference, Edinburgh, (2008), pp.1-30.
- [30] Lopes. M. J. and Lopes. M. L. 1999, "Soil-Synthetic Interaction-Influence of Soil Particle Size and Geosynthetic Structure". Geosynthetics International, Vol. 6, No. 4, pp. 261-282.